iJRASET
International Journal For Research in Applied Science and Engineering Technology

INTERNATIONAL JOURNAL FOR RESEARCH

IN APPLIED SCIENCE & ENGINEERING TECHNOLOGY

Volume: 13 **Issue:** VIII **Month of publication:** August 2025

DOI: https://doi.org/10.22214/ijraset.2025.73513

www.ijraset.com

Call: 08813907089 | E-mail ID: ijraset@gmail.com

International Journal for Research in Applied Science & Engineering Technology (IJRASET)
ISSN: 2321-9653; IC Value: 45.98; SJ Impact Factor: 7.538
Volume 13 Issue VIII Aug 2025- Available at www.ijraset.com

Performance Analysis of a Three-Tube Serpentine Receiver in a Parabolic Trough Solar Collector for Domestic Applications

Mr. Krishna Yadav[1], Mr. Mrigendra Singh[2], Ms. Priyanka Malviya[3]
Department of Mechanical Engineering, Sushila Devi Bansal College of Technology, Indore, 453331, India

Abstract: Abstract: This paper investigates the optical and thermal performance of a parabolic trough solar collector integrated with a three-tube serpentine absorber. Driven by the increasing demand for efficient and compact solar thermal systems for domestic applications, this configuration aims to overcome the limitations of traditional single-tube receivers, such as limited residence time and uneven temperature distribution. Employing a combined simulation methodology, including three-dimensional ray tracing in COMSOL Multiphysics for optical simulation and conjugate heat transfer simulations in ANSYS Fluent for fluid temperature analysis, the study evaluates performance under four focal alignment conditions (100%, 90%, 80%, and 70%) to replicate real-world solar tracking variations. Findings indicated that multi-tube serpentine receivers provided significantly better thermal uniformity, higher outlet temperatures, and improved tolerance to optical misalignment compared to the single-tube design, making it a viable option for compact solar preheating systems.

Keywords: Parabolic Trough Collector, Serpentine Tube Absorber, Optical Simulation, Sun Ray Tracing, Thermal Analysis, Three-tube Receiver.

I. INTRODUCTION

The global shift towards renewable energy is an urgent necessity driven by concerns over fossil fuel depletion, increasing carbon dioxide emissions, and environmental degradation. Solar energy, with its abundance and universal availability, stands out as a promising alternative. Solar thermal systems are particularly well-suited for domestic applications requiring low-to-medium temperatures (typically below 100°C), such as water heating[1]. Among various solar thermal technologies, Parabolic Trough Collectors have matured into effective systems, concentrating solar radiation onto a receiver tube to heat a working fluid. While historically used in large-scale power plants, there is a growing interest in adapting PTCs for domestic use, necessitating compact and efficient designs[2].

Traditional straight-tube PTC receivers face challenges such as limited heat exchange surface area and fluid residence time, which can hinder their efficiency in compact, low-flow domestic systems[3]. To address these limitations, multi-tube serpentine designs are being explored to enhance thermal performance. Serpentine tubes, widely used in heat exchangers, increase fluid residence time, promote secondary flow patterns for better mixing, and improve convective heat transfer, leading to more uniform temperature distribution[4][5].

The objective is to analyze its optical and thermal performance under varying focal alignment conditions, providing insights into its suitability for domestic thermal applications. This research builds upon existing literature that highlights the importance of optimizing receiver tube design and leveraging computational fluid dynamics to simulate real-world performance under varying flow conditions and heat flux distributions.

II. SYSTEM DESIGN AND MODELING

The three-tube serpentine receiver was designed as part of a parabolic trough solar collector system[6]. The overall PTC system relies on a parabolic reflector to concentrate solar radiation onto a linear receiver at its focal line. The parabolic reflector in this design has an aperture width of 1220 mm and an aperture length of 1668 mm, with a focal length of 606.5 mm and a rim angle of 67°. The reflector material is polished aluminium, selected for its high reflectivity, and the absorber tubes are made of copper for excellent thermal conductivity.

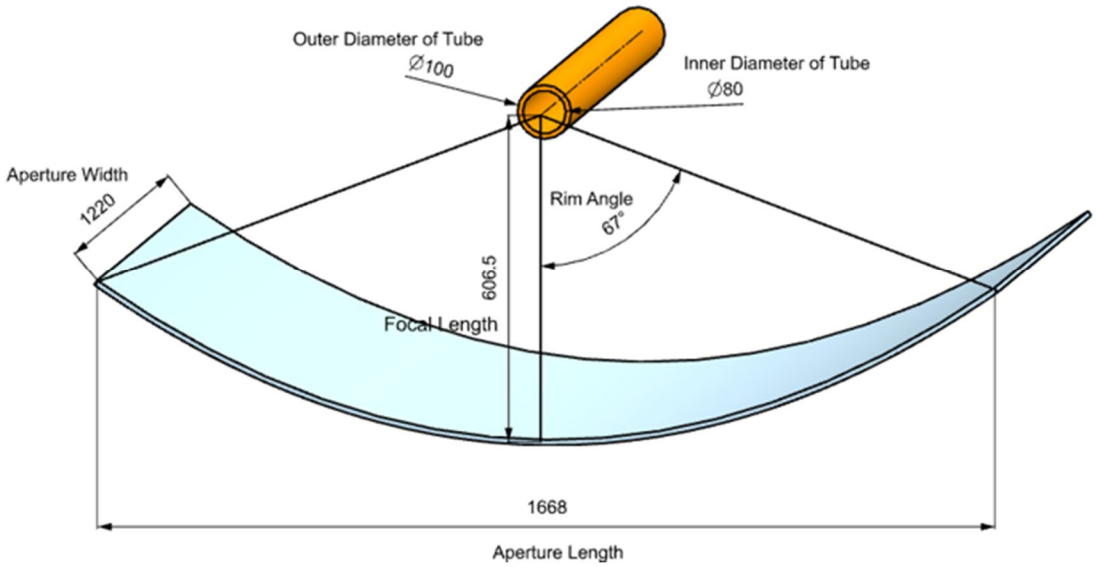

Figure 1: CAD model of Parabolic trough geometry with receiver design

A. Three-Tube Absorber Design

The three-tube absorber configuration was developed to increase the surface area and fluid residence time for better heat transfer compared to a single-tube design[7]. The design consists of a main tube (MT) and two preheater tubes, named Left Preheater Tube 1 (LPT 1) and Right Preheater Tube 1 (RPT 1). The tubes are arranged in parallel serpentine segments, allowing a distributed thermal load. The internal volume of this configuration is approximately 9,946,283 mm³ (or about 10 liters). The fluid flow direction is designed such that the inlet flow divides into two paths, each following a serpentine trajectory, rejoining at the outlet. The outer diameter for the main absorber tube is 100 mm, with an inner diameter of 80 mm. The preheater tubes have an outer diameter of 40 mm and an inner diameter of 30 mm.

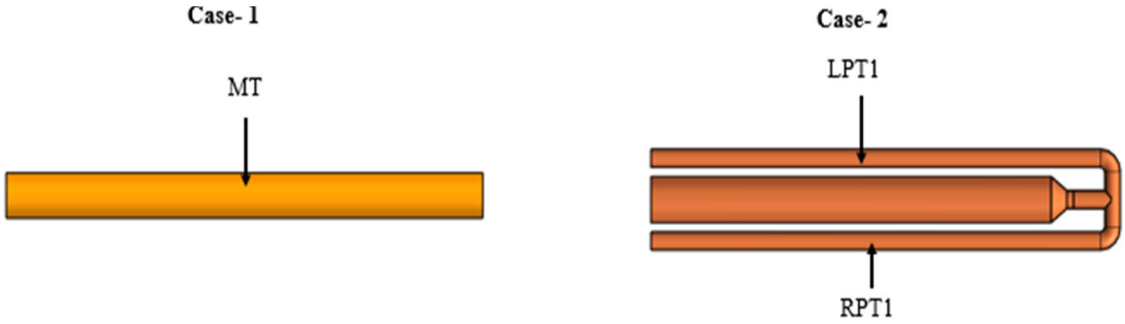

Figure 1: CAD model of Absorber tubes

B. Absorber Tube Placement at Different Focal Lengths

To simulate real-world solar tracking variations and mechanical misalignments, each absorber tube configuration, including the three-tube design, was modeled at four different focal distances from the vertex of the reflector. These variations were parametrically modeled using Siemens NX to ensure dimensional consistency.

The vertical positioning of the absorber array was altered according to percentages of the nominal focal length (606.5 mm):

Case 2A: 100% Focal Length – Tube center placed at 606.5 mm

Case 2B: 90% Focal Length – Tube center placed at 546 mm

Case 2C: 80% Focal Length – Tube center placed at 485 mm

Case 2D: 70% Focal Length – Tube center placed at 424.5 mm

The tube shapes, diameters, and serpentine layouts remained constant within each configuration across all focal cases to ensure fair comparison.

C. Boundary Conditions and Simulation Parameters

The simulations were set up in COMSOL Multiphysics and ANSYS Fluent with consistent boundary conditions for all cases. The inlet water temperature was set to 300 K, and the inlet water velocity was 0.03 m/s. The concentrated rate on the lower surface of the single tube (reference configuration) was 8817 W/m², and the direct normal solar energy on the upper surface was 589 W/m². A laminar turbulence model was selected as the flow was within the low-Reynolds number range. No-slip conditions were applied at fluid-solid interfaces, and the outlet pressure was set to atmospheric (gauge pressure = 0).

III. OPTICAL SIMULATION AND THERMAL ANALYSIS

The study employed a sequential multi-domain simulation approach to evaluate the optical and thermal performance of the three-tube serpentine PTC system. The entire analysis was conducted within a Multiphysics environment to accurately represent real-world solar collector behaviour.

A. Ray Tracing Simulation

Three-dimensional ray tracing simulations were performed using the COMSOL Ray Optics Module. The 3D geometry from Siemens NX was imported, and solar rays were defined as a parallel beam, representative of direct normal irradiance during midday solar conditions. The parabolic mirror was assigned a mirror boundary condition with 90% reflectivity, while the absorber tubes were treated as opaque surfaces that capture ray intersections[8][9]. The purpose of this stage was to map the spatial distribution of solar energy on the absorber surfaces, capturing how light interacts with the non-planar serpentine tubes and any lateral dispersion effects.

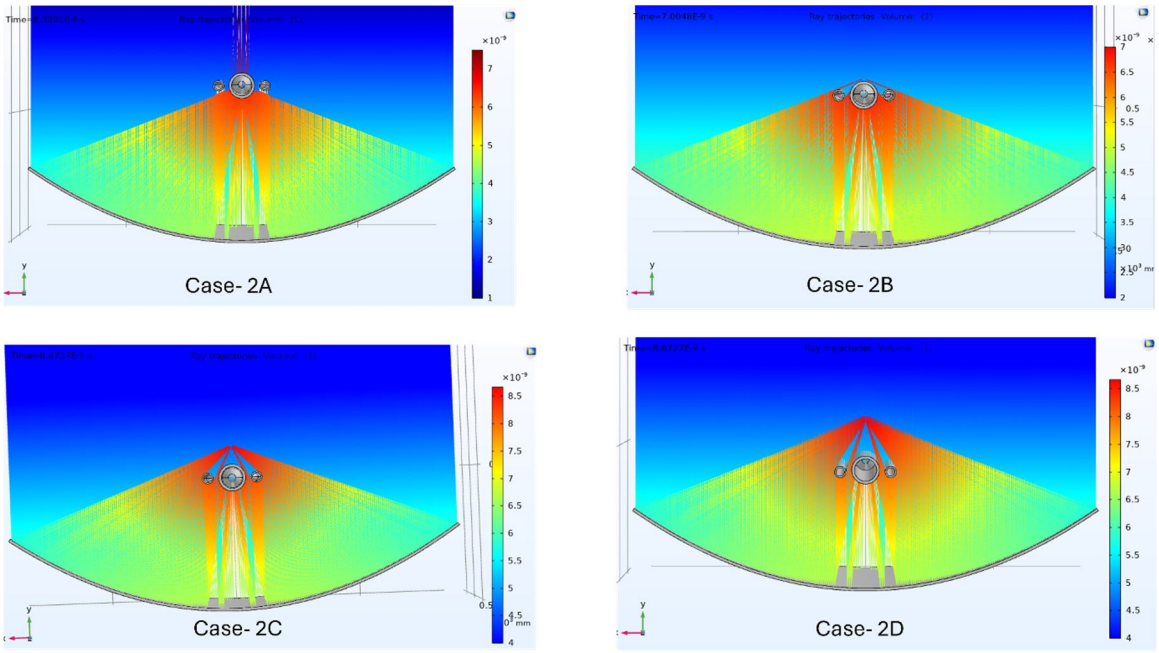

Figure 1: Ray tracing results for Three-tube configuration

Case 2A: Rays are distributed across all three tubes. The central tube receives the highest concentration, while side tubes receive negligible rays, causing no preheating. Alignment is geometrically optimized.
Case 2B: Slight defocusing shifts the ray impact, but the three-tube spread helps capture rays effectively. The ray pattern begins to shift downward relative to the tube centers.
Case 2C: Further misalignment causes reduced precision in ray targeting. Some rays fall between the tubes, but energy interception is partially maintained due to the multi-tube arrangement.
Case 2D: The focus line falls well below the tube array. Although misalignment is evident, the wider distribution of tubes allows some rays to still be intercepted by outer tubes.

ISSN: 2321-9653; IC Value: 45.98; SJ Impact Factor: 7.538
Volume 13 Issue VIII Aug 2025- Available at www.ijraset.com

B. Heat Flux Distribution

Following the ray tracing simulation, the ray intersection data was converted into surface heat flux distributions across the absorber tubes.

The incident radiant flux (q) was calculated as a function of angular position on the tube surface, using:

$$q(\theta) = I \cdot \rho \cdot \cos(\theta_i) / A$$

This process defined the quantity and spatial variation of energy absorbed per unit area of the receiver surface, serving as the applied thermal load for subsequent heat transfer simulations[10][11]. In Solidworks's flow simulation and thermal analysis environment, local incident energy values were generated and projected onto the outer surfaces of the absorber tubes.

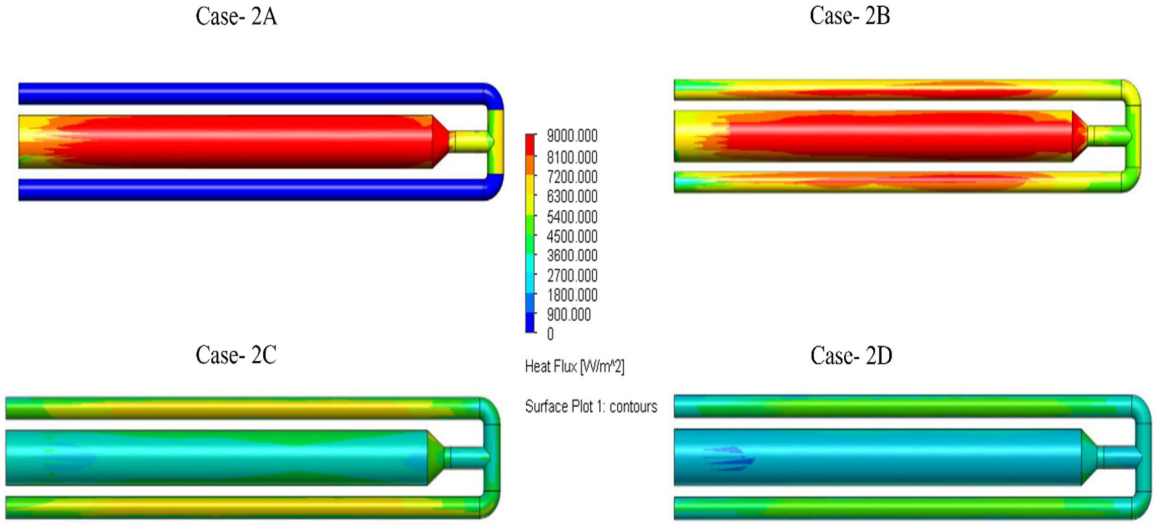

Figure 2: Heat flux distribution on Lower Surface of absorber for Case-2

Case 2A: The rays focus centrally on the middle tube, with symmetrical dispersion across the three-tube array. The middle tube receives the highest heat flux, denoted by the solid red band, while adjacent tubes show decreasing values. The outer tubes receive secondary radiation, reducing thermal losses and improving the collector's net effectiveness.

Case 2B: Slight optical deviation causes the focal point to shift laterally, distributing heat unevenly across the three tubes. The flux peak moves off-center but still covers a large portion of the array. The central tube continues to receive significant energy, while neighbouring tubes see increased absorption due to the wider spread.

Case 2C: Further reduction in focus alignment causes diminished intensity and an expanded distribution of rays across all three tubes. The red and yellow flux zones diminish, giving way to green and light blue bands, especially in the outer tubes.

Case 2D: This case exhibits broad and diffused solar ray impact across the entire collector, with most energy falling outside the tube surfaces. Flux intensity is considerably reduced and spread thinly across the tube surfaces, visible in light green and cyan contours.

The heat flux profiles were inherently non-uniform due to the curved geometry of the parabolic mirror and the 3D nature of the simulation. Concentration was generally higher near the top-facing surfaces, decreasing toward the sides and bottom. In the three-tube system, flux was distributed across multiple surfaces. The external surfaces were discretized into patches to allow precise application of spatially-resolved energy input.

C. Thermal-Fluid Analysis

The final stage involved performing a Conjugate Heat Transfer analysis in ANSYS Fluent to evaluate the temperature distribution within the working fluid domain[12]. The fluid and solid domains of the absorber tube assemblies were imported from Siemens NX into ANSYS Workbench[13]. The outer wall of the solid domain received the non-uniform surface heat flux data extracted from the COMSOL ray optics simulation, applied as a spatially varying boundary condition[14]. The outlet temperature (T_{out}) was computed using the energy balance:

$$mc_p(T_{out} - T_{in}) = q \cdot A_{abs}$$

Heat transfer through the copper tube wall was modeled via conduction, and convective heat transfer to the water was resolved through Navier-Stokes energy equations.

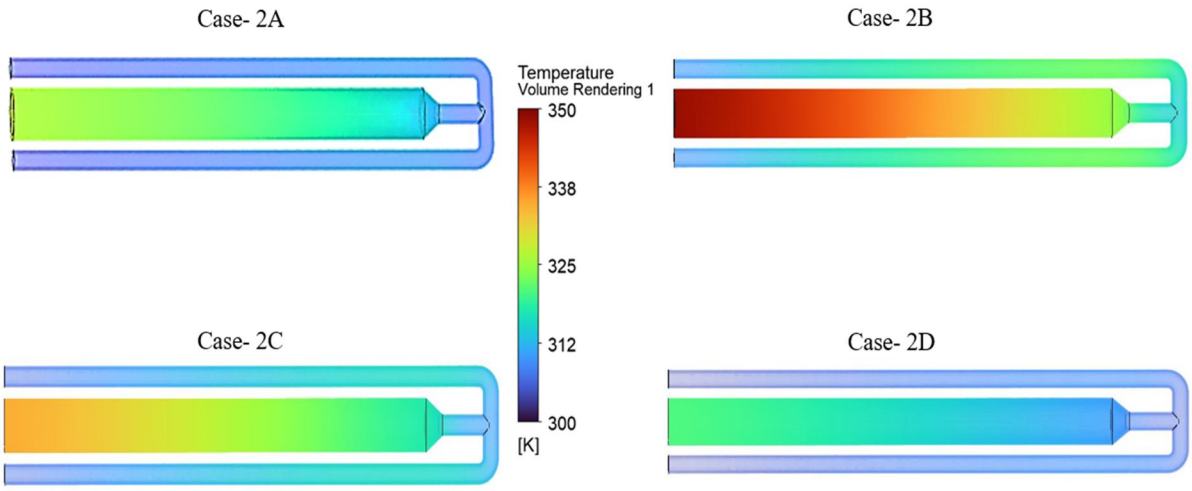

Figure 3: Temperature distribution in absorber Tube for Case-2

Case 2A: The serpentine routing clearly influences thermal development. Inlet zones remain cooler (blue to green), but central zones, particularly the mid-sections, show higher intensity (yellow to red). The heating is non-linear due to flow redirection and varying local flux inputs, creating localized temperature bands along the active segments.

Case 2B: The central zones show even higher intensity, with a significant portion of the main tube (MT) turning red, indicating temperatures reaching 338 K and above. The preheater tubes (LPT1 and RPT1) also show a more pronounced temperature increase (yellow-orange zones) compared to Case 2A.

Case 2C: The intensity decreases, but the overall temperature increase throughout the serpentine path is still evident, with extended yellow-green regions across all tubes. The distribution is more spread out, showcasing the effect of broader ray interception.

Case 2D: The temperature increase is significantly lower compared to the other focal alignments, with most of the tubes remaining in the blue-green range. This indicates less efficient energy capture due to significant misalignment, but still demonstrates some thermal gain.

IV. RESULTS AND DISCUSSION

The detailed ray tracing and thermal-fluid simulations provided comprehensive insights into the performance of the three-tube serpentine receiver.

A. Angular Solar Heat Flux Distribution

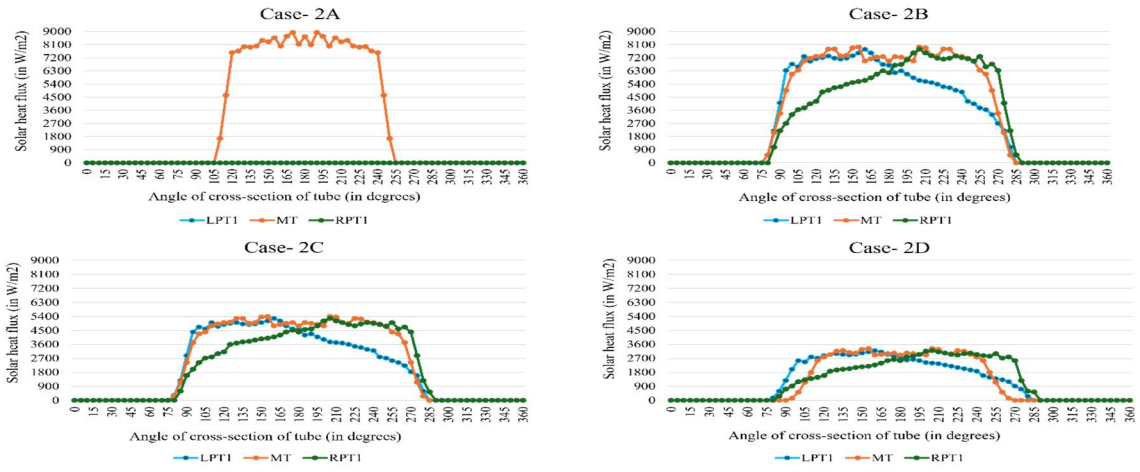

Figure 4: Angular Distribution of Reflected Solar Heat Flux on Tube Surface for Case-2

Case 2A: At perfect focus, peak flux is largely captured by the central tube (MT), while lateral tubes (LPT1 and RPT1) receive negligible heat due to sharp optical convergence. The MT shows a sharp peak in heat flux, reaching around 8500-8800 W/m².
Case 2B: As focus is reduced, heat flux begins to spread towards LPT1 and RPT1, enhancing uniformity across all pipes. Tube 2 still dominates, but LPT1 and RPT1 receive about 70% of the peak flux, indicating better shared energy absorption. The peaks are lower and broader for all tubes compared to the 100% focus case.
Case 2C: The heat flux distribution becomes even more spread out and the peak values for all tubes are further reduced. The three tubes receive a more balanced, albeit lower, amount of solar energy, demonstrating the system's ability to distribute the thermal load under misalignment.
Case 2D: At this level of misalignment, the flux profile is significantly flattened and reduced in magnitude across all three tubes. The energy is highly diffused, but the multi-tube configuration still allows for some energy interception, preventing complete loss of performance.
This progression shows that while ideal focus concentrates energy intensely on the main tube, slight defocusing allows the multi-tube configuration to effectively spread the thermal load[15]. This distributed absorption pattern is beneficial for spreading thermal stress and increasing the effective area of heating.

B. Temperature Contour Analysis and Outlet Temperatures

The thermal simulation results, processed using ANSYS Fluent, provide volume-averaged temperature profiles for the working fluid[16]. The thermal efficiency (η) was calculated as:

$$\eta = mc_p(T_{out} - T_{in}) / I \cdot A_{ap}$$

The thermal efficiency is calculated using the energy balance equation. For Case-2B (90% focus):
$m^{\cdot}$ = 0.03 kg/s, cp = 4180 J/kg·K, T_{out} = 340 K, T_{in} = 300 K
q = 7000W/m^2, Aabs = 0.1 m^2

$$mc_p(T_{out} - T_{in}) = 0.03 \cdot 4180 \cdot (340 - 300) = 5016W$$
$$\eta = 5016 / 1000 \cdot 2.64 \approx 0.728 \text{ or } 72.8\%$$

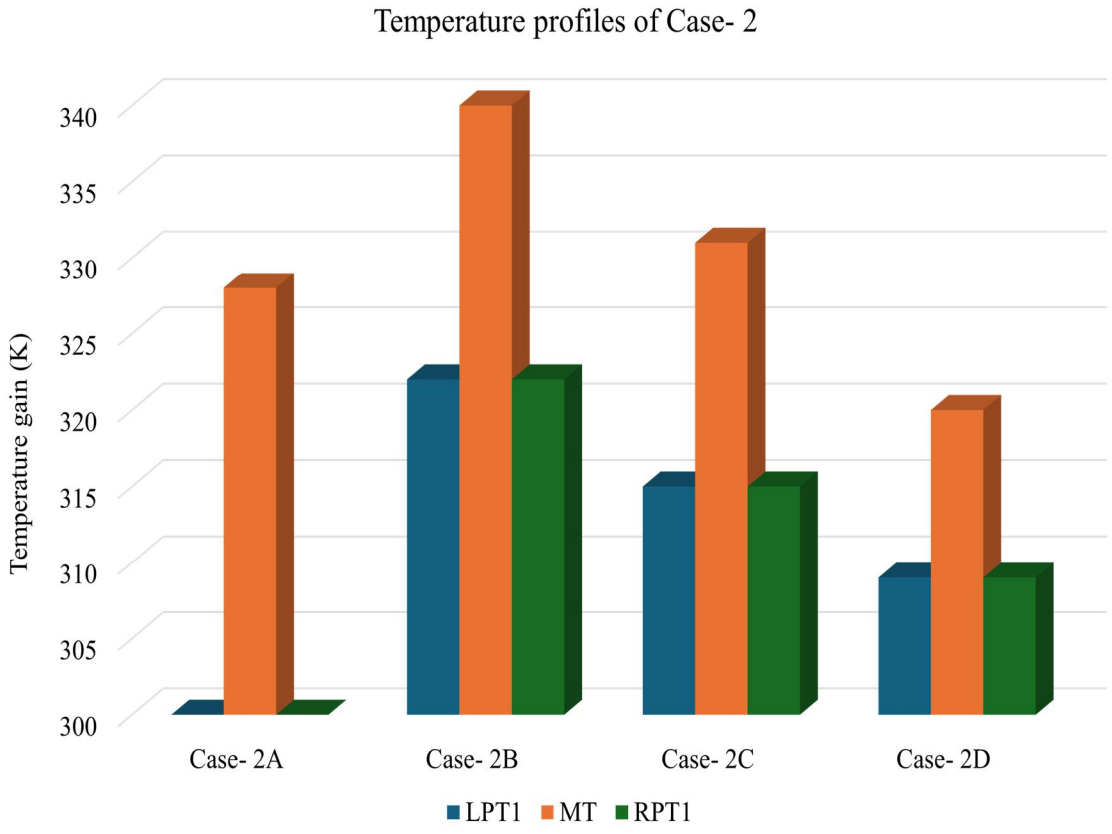

Figure 5: Performance comparison of receiver tube cases for Case- 1

For the Case 2, the Main Tube (MT) exhibits the highest temperature under all conditions, confirming its role as the primary heat recipient. At 90% focus (Case 2B), the MT reaches an outlet temperature exceeding 340, which is higher than the single-tube case, indicating enhanced performance due to energy redistribution. The preheater tubes (LPT1 and RPT1) show moderate heating (around 320–322 K, represented by the blue and green bars respectively), demonstrating effective thermal spreading. The temperature disparity between MT and LPT1/RPT1 reduces with decreasing focus percentage, highlighting more uniform energy dispersion. This suggests that the three-tube configuration is more robust to focal misalignment compared to the single-tube design.

V. CONCLUSION

This study successfully investigated the optical concentration efficiency and thermal performance of a parabolic trough solar collector integrated with a three-tube serpentine absorber under various focal alignment conditions. The combined modeling approach using Siemens NX, COMSOL Multiphysics, and ANSYS Fluent effectively linked geometric design, solar flux behaviour, and fluid temperature distribution.

The ray tracing simulations confirmed that while perfect focal alignment leads to highly concentrated solar flux on the central tube, this configuration also benefits from the spreading of reflected rays under slight misalignment. The three-tube design demonstrated better tolerance to optical misalignment by capturing a broader portion of the distributed rays, thereby improving system resilience. The thermal analysis revealed that the three-tube configuration, particularly at 90% focal alignment, achieved high outlet temperatures in the main tube while effectively preheating the fluid in the adjacent serpentine paths. This indicates that the multi-tube serpentine geometry not only enhances heat transfer but also provides structural and operational robustness under realistic solar tracking errors.

The three-tube serpentine receiver offers tangible advantages, including improved fluid residence time, volumetric heating, and distributed flux absorption, contributing to better thermal management. Its efficiency even at suboptimal focus makes it well-suited for real-world conditions where solar incidence varies throughout the day.

VI. ACKNOWLEDGMENT

The authors would like to thank the Department of Mechanical Engineering, Sushila Devi Bansal College of Technology, for providing the simulation resources and technical support essential for this study. Special appreciation is extended to the faculty and laboratory staff for their assistance with CAD modeling and thermal-fluid simulation tools. The authors are also grateful to the reviewers for their valuable feedback that helped improve the quality of this research.

REFERENCES

[1] “India Energy Outlook 2021 – Analysis - IEA.” Accessed: Jun. 30, 2025. [Online]. Available: https://www.iea.org/reports/india-energy-outlook-2021
[2] S. Kalogirou, “Thermal performance, economic and environmental life cycle analysis of thermosiphon solar water heaters,” Solar Energy, vol. 83, no. 1, pp. 39–48, Jan. 2009, doi: 10.1016/J.SOLENER.2008.06.005.
[3] A. Bilal Awan, M. N. Khan, M. Zubair, and E. Bellos, “Commercial parabolic trough CSP plants: Research trends and technological advancements,” Solar Energy, vol. 211, pp. 1422–1458, Nov. 2020, doi: 10.1016/j.solener.2020.09.072.
[4] N. S. Lewis and D. G. Nocera, “Powering the planet: Chemical challenges in solar energy utilization,” Proc Natl Acad Sci U S A, vol. 103, no. 43, pp. 15729–15735, Oct. 2006, doi: 10.1073/PNAS.0603395103/ASSET/3DE8043E-D8A1-44B0-AFD0-FD0C4CC001CE/ASSETS/GRAPHIC/ZPQ03906360600E4.JPEG.
[5] Y. Tian and C. Y. Zhao, “A review of solar collectors and thermal energy storage in solar thermal applications,” Appl Energy, vol. 104, pp. 538–553, 2013, doi: 10.1016/j.apenergy.2012.11.051.
[6] İ. H. Yılmaz and A. Mwesigye, “Modeling, simulation and performance analysis of parabolic trough solar collectors: A comprehensive review,” Appl Energy, vol. 225, pp. 135–174, Sep. 2018, doi: 10.1016/j.apenergy.2018.05.014.
[7] E. Bellos and C. Tzivanidis, “Alternative designs of parabolic trough solar collectors,” Prog Energy Combust Sci, vol. 71, pp. 81–117, Mar. 2019, doi: 10.1016/J.PECS.2018.11.001.
[8] H. Liang, S. You, and H. Zhang, “Comparison of different heat transfer models for parabolic trough solar collectors,” Appl Energy, vol. 148, pp. 105–114, Jun. 2015, doi: 10.1016/J.APENERGY.2015.03.059.
[9] H. Liang, S. You, and H. Zhang, “Comparison of three optical models and analysis of geometric parameters for parabolic trough solar collectors,” Energy, vol. 96, pp. 37–47, Feb. 2016, doi: 10.1016/J.ENERGY.2015.12.050.
[10] J. Akhatov, K. Akhmadov, and N. Juraboyev, “Thermal performance enhancement in the receiver part of solar parabolic trough collectors,” UNEC journal of engineering and applied sciences, vol. 3, no. 2, pp. 5–13, Dec. 2023, doi: 10.61640/UJEAS.2023.1201.
[11] Y. L. He, K. Wang, Y. Qiu, B. C. Du, Q. Liang, and S. Du, “Review of the solar flux distribution in concentrated solar power: Non-uniform features, challenges, and solutions,” Appl Therm Eng, vol. 149, pp. 448–474, Feb. 2019, doi: 10.1016/j.applthermaleng.2018.12.006.
[12] J. Muñoz and A. Abánades, “Analysis of internal helically finned tubes for parabolic trough design by CFD tools,” Appl Energy, vol. 88, no. 11, pp. 4139–4149, Nov. 2011, doi: 10.1016/J.APENERGY.2011.04.026.

[13] A. M. De Oliveira Siqueira, P. E. N. Gomes, L. Torrezani, E. O. Lucas, and G. M. Da Cruz Pereira, "Heat Transfer Analysis and Modeling of a Parabolic Trough Solar Collector: An Analysis," Energy Procedia, vol. 57, pp. 401–410, Jan. 2014, doi: 10.1016/J.EGYPRO.2014.10.193.
[14] S. E. Ghasemi and A. A. Ranjbar, "Thermal performance analysis of solar parabolic trough collector using nanofluid as working fluid: A CFD modelling study," J Mol Liq, vol. 222, pp. 159–166, Oct. 2016, doi: 10.1016/J.MOLLIQ.2016.06.091.
[15] S. A. Kalogirou, S. Lloyd, J. Ward, and P. Eleftheriou, "Design and performance characteristics of a parabolic-trough solar-collector system," Appl Energy, vol. 47, no. 4, pp. 341–354, Jan. 1994, doi: 10.1016/0306-2619(94)90041-8
[16] M. Singh, M. K. Sharma, and J. Bhattacharya, "Design methodology of a parabolic trough collector field for maximum annual energy yield," Renew Energy, vol. 177, pp. 229–241, Nov. 2021, doi: 10.1016/J.RENENE.2021.05.102.

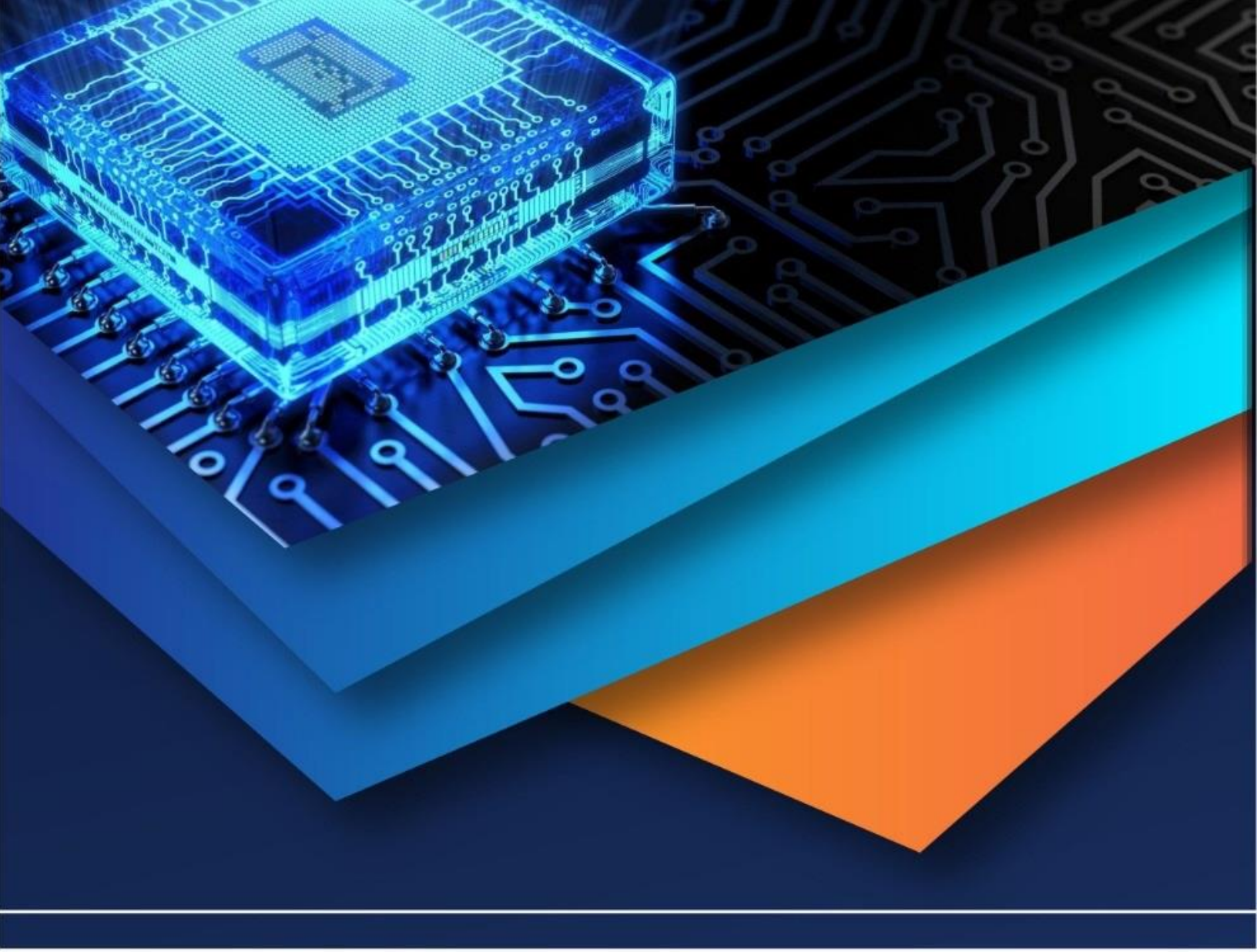

10.22214/IJRASET

45.98

IMPACT FACTOR: 7.129

IMPACT FACTOR: 7.429

INTERNATIONAL JOURNAL FOR RESEARCH

IN APPLIED SCIENCE & ENGINEERING TECHNOLOGY